Title:

Tat proteins as novel thylakoid membrane anchors organize a biosynthetic pathway in chloroplasts and increase product yield 4-fold

Author affiliation:

Maria Perestrello Ramos Henriques de Jesus[a], Agnieszka Zygadlo Nielsen[a], Silas Busck Mellor[a], Annemarie Matthes[a], Meike Burow[b], Colin Robinson[c], Poul Erik Jensen[a]

[a]Copenhagen Plant Science Center, Center for Synthetic Biology "bioSYNergy", Department of Plant and Environmental Sciences, University of Copenhagen, Thorvaldsensvej 40, DK-1871 Frederiksberg C, Denmark

[b]DynaMo Center, Department of Plant and Environmental Sciences, University of Copenhagen, Thorvaldsensvej 40, 1871 Frederiksberg C, Denmark

[c]School of Biosciences, University of Kent, Canterbury CT2 7NJ, UK

Corresponding Author:

Poul Erik Jensen

Copenhagen Plant Science Center, Center for Synthetic Biology "bioSYNergy", Department of Plant and Environmental Sciences, University of Copenhagen, Thorvaldsensvej 40, DK-1871 Frederiksberg C, Denmark

+45 6134 4637

peje@plen.ku.dk

Abstract

Photosynthesis drives the production of ATP and NADPH, and acts as a source of carbon for primary metabolism. NADPH is also used in the production of many natural bioactive compounds. These are usually synthesized in low quantities and are often difficult to produce by chemical synthesis due to their complex structures. Some of the crucial enzymes catalyzing their biosynthesis are the cytochromes P450 (P450s) situated in the endoplasmic reticulum (ER), powered by electron transfers from NADPH. Dhurrin is a cyanogenic glucoside and its biosynthesis involves a dynamic metabolon formed by two P450s, a UDP-glucosyltransferase (UGT) and a P450 oxidoreductase (POR). Its biosynthetic pathway has been relocated to the chloroplast where ferredoxin, reduced through the photosynthetic electron transport chain, serves as an efficient electron donor to the P450s, bypassing the involvement of POR. Nevertheless, translocation of the pathway from the ER to the chloroplast creates other difficulties, such as the loss of metabolon formation and intermediate diversion into other metabolic pathways. We show here that co-localization of these enzymes in the thylakoid membrane leads to a significant increase in product formation, with a concomitant decrease in off-pathway intermediates. This was achieved by exchanging the membrane anchors of the dhurrin pathway enzymes to components of the Twin-arginine translocation pathway, TatB and TatC, which have self-assembly properties. Consequently, we show 4-fold increased titers of dhurrin and a decrease in the amounts of intermediates and side products in *Nicotiana benthamiana*. Further, results suggest that targeting the UGT to the membrane is a key factor to achieve efficient substrate channeling.

Keywords

Substrate channeling; twin-arginine translocation pathway; dhurrin; fusion proteins; light-driven; chloroplast

Highlights

- Fusion of Tat proteins to the enzymes of the dhurrin pathway *in Nicotiana benthamiana* leads to efficient substrate channeling.
- Cytochrome P450s are functional after exchange of membrane anchors with components of the Tat pathway
- Targeting the UGT to the membrane is a key factor in substrate channeling.
- Re-organization of the pathway leads to a 4-fold increase in dhurrin production and decrease in the amounts of intermediates and side-products.

Introduction

Metabolic engineering has become an attractive alternative to synthetic chemistry due to the promise of producing a range of compounds, from high-value specialty compounds such as therapeutics to bulk commodities including plastics and biofuels, in a cheap and renewable manner. Many such specialty compounds are plant natural products whose biosynthesis requires enzymes termed cytochromes P450 (P450s). These are heme-containing monooxygenases that catalyze regio- and stereo-specific hydroxylations often difficult to perform by chemical synthesis. In eukaryotes, P450s localize to the endoplasmic reticulum (ER) and require a NADPH-dependent reductase to provide electrons as reducing power [1–3].

Dhurrin (*D*-glucopyranosyloxy-(S)-*p*-hydroxymandelonitrile) is a cyanogenic glucoside used as a defense compound by *Sorghum bicolor* and has served as a model pathway to study the coupling of heterologously expressed P450s to photosynthetic electron transport[4–8]. The pathway consists of two ER membrane-bound cytochrome P450 enzymes (CYP79A1 and CYP71E1) and a soluble UDP-glucosyltransferase (UGT85B1), which catalyzes the step-wise conversion of tyrosine to dhurrin (Fig. 1a). CYP79A1 converts L-tyrosine to *(Z)-p*-hydroxyphenylacetaldoxime (oxime), which is converted into the cyanohydrin *p*-hydroxymandelonitrile (nitrile) by CYP71E1. Lastly, UGT85B1 stabilizes the nitrile by glucosylation to yield dhurrin [9–11]. Since the nitrile is labile at neutral and alkaline pH it dissociates into HCN and *p*-hydroxybenzaldehyde (aldehyde) if not rapidly glucosylated[12]. These enzymes were recently shown to form a dynamic metabolon together with the cytochrome P450 oxidoreductase (POR), that efficiently channels the substrate into the final product [13], thereby avoiding this unwanted side-reaction.

The dhurrin pathway can be relocated to the chloroplast where ferredoxin, reduced through photosynthesis, serves as an efficient electron donor to the P450s [4], bypassing the involvement of POR [14,15]. Nonetheless, the relocation of entire pathways is often associated with issues such as the disruption of endogenous complexes that might lead to leakage of potentially toxic and/or unstable intermediates that can be secreted or diverted into other metabolic pathways, leading to reduced yields[16–19]. Expression of the dhurrin pathway in the ER of *Arabidopsis* and tobacco [20,21] and also tobacco chloroplasts [5] shows the presence of a plethora of metabolites derived from pathway intermediates. These are formed with concomitant release of toxic hydrogen cyanide, and represent a loss of carbon that otherwise would be channeled into the final product. The formation of enzyme complexes in living cells plays a key role in controlling

the channeling of metabolic fluxes towards specific targets [17]. Engineering enzymes into close proximity creates a microenvironment where intermediates can be channeled directly between enzymes, which in turn avoids free diffusion and cross talk with other pathways and increases overall product yields [16,18]. Here we attempt to improve channeling of tyrosine into dhurrin by using subunits of the ΔpH-dependent twin-arginine translocation (Tat) complex as a scaffold. The Tat complex is responsible for the active translocation of folded proteins across a lipid bilayer in plant thylakoids and prokaryotes [22,23]. It comprises three essential proteins: TatA, TatB and TatC, but sometimes includes additional proteins, which arise from gene duplication of TatA[23]. The TatB and TatC protein components interact with each other to form a heterodimer and the native TatBC complex contains several copies of TatBC. In *E. coli*, TatB comprises an N-terminal transmembrane helix followed by a basic amphipathic helix. The central region of the protein is predicted to be mainly helical, and the C-terminal region to be in a random coiled conformation [24,25]. The transmembrane domain has been reported as the contact site between TatB and the transmembrane helix 5 of TatC [26–28]. However, the amphipathic helix was also shown to have peripheral interactions with the membrane [29]. Moreover, bacterial two-hybrid analysis of the TatB protein, showed that besides the transmembrane domain and the amphipathic helix, its central region is still important for it to self-interact [24].

Co-localization of the dhurrin pathway enzymes was achieved by exchanging the natural membrane anchors of the P450s with TatB and fusing the soluble UGT to the transmembrane protein TatC via a flexible linker. Using this approach we show improved substrate channeling, reduced formation of side products, and consequently increased dhurrin titers in transient infiltration of *Nicotiana benthamiana*.

Results:

Design of fusion proteins:

We hypothesized that the Tat proteins could be used to bring the dhurrin pathway enzymes into close proximity, improving substrate channeling and product yields. To test this, we fused the CYP79A1, CYP71E1 and UGT85B1 with the membrane spanning parts of *Arabidopsis* Tat proteins (Fig.1).

As controls, the native enzymes from *Sorghum bicolor* were fused to the transit peptide from ferredoxin (TP_{Fd}) in order to target the proteins to the chloroplast. This is cleaved once the proteins enter the chloroplast and should have no effect on protein activity.

Two different P450-TatB fusions were constructed for each P450 enzyme (BS-79, BS-71, BL-79, and BL-71) with the TatB from *A. thaliana*. A short (prefix BS-) version, which contains the transit peptide, predicted transmembrane domain and amphipathic helix considered to be responsible for the assembly of TatB and TatC, and a long (prefix BL-) version, which additionally includes the central region of the protein, important for TatB-TatB interaction. The natural transmembrane helix domain of the P450s was removed before fusing the TatB parts.

TatC is a six transmembrane domain protein whose fifth helix is responsible for interaction with TatB [26,27]. Since keeping only the fifth helix could lead to misfolding and possible proteolysis, we fused the entire TatC protein, including the transit peptide, to UGT85B1. As this UGT is a soluble protein, a 15 amino acid linker was added to ensure flexibility. For that purpose a Gly/Ser sequence was chosen to avoid secondary structure and reduce susceptibility to proteases [30]. In case of the Tat fusions, the transit peptide from ferredoxin was unnecessary, since both TatB and TatC possess their own transit peptides, which direct them to the chloroplast.

Transient infiltration of plants allows for high protein expression and is a quick and simple method for combinatorial studies [31,32]. *Agrobacterium* cells transformed with the expression vectors carrying single constructs were generated. Subsequently, single or mixtures of different cultures of *Agrobacterium* were infiltrated in *N. benthamiana* leaves to generate plants that transiently expressed the different fusion constructs.

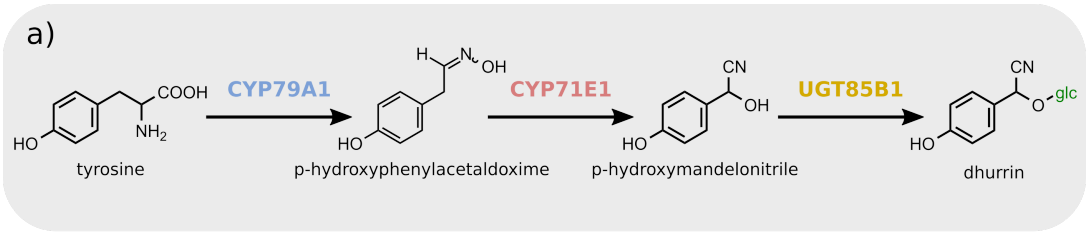

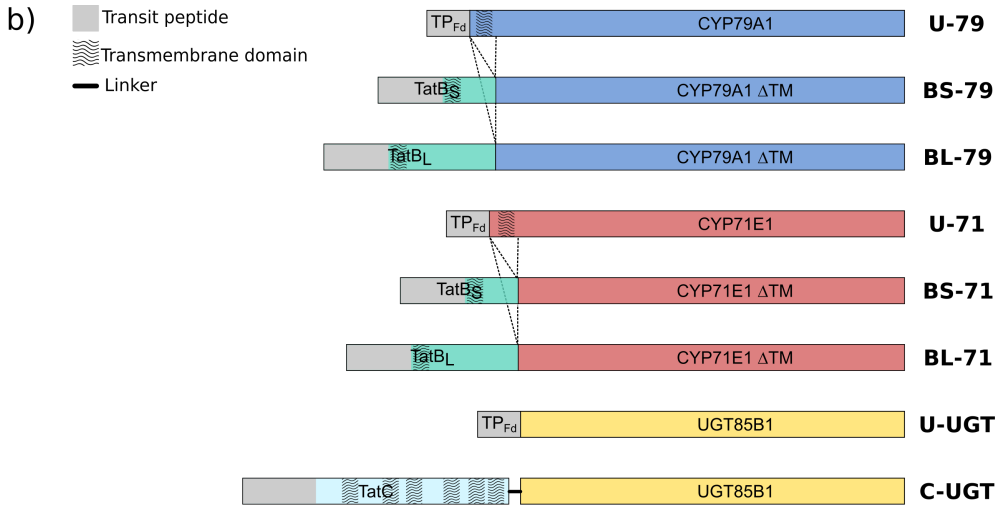

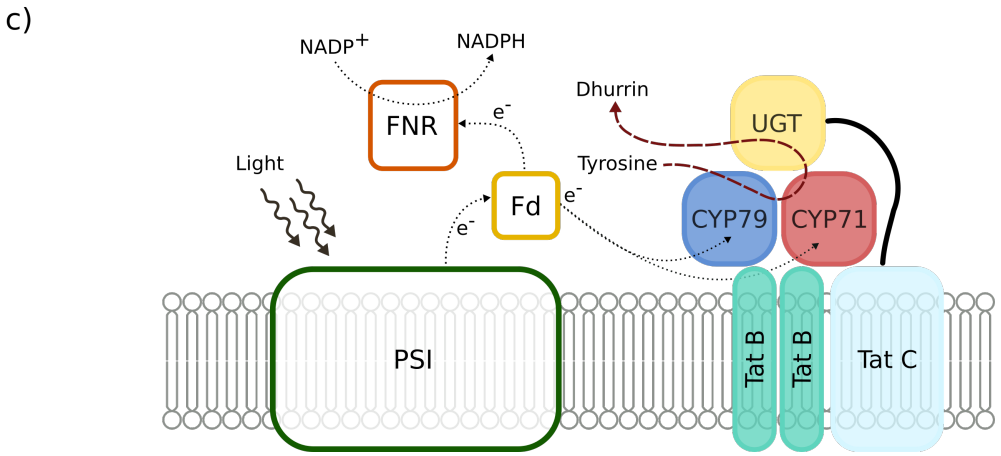

Fig. 1. Schematic representation of the dhurrin pathway, the fusion enzymes engineered and its organization in the thylakoids. **a)** The dhurrin pathway consists of two membrane-bound P450s (CYP79A1 and CYP71E1) and a soluble UDP-glucosyl transferase (UGT85B1). **b)** Construct design of fusion enzymes generated. The transit peptide from ferredoxin (TP_{Fd}) was fused to the cDNA encoding the native enzymes from *S. bicolor*: CYP79A1 (U-79), CYP71E1 (U-71) and UGT85B1 (U-UGT). Further the P450s without their transmembrane domains (CYP79A1: Δ1-105 and CYP71E1: Δ1-111) were fused to two different lengths of the cDNA encoding the membrane spanning and interacting part of the TatB protein from *A. thaliana*: TatB short – Δ151-260 (TatBS) and TatB long – Δ220-260 (TatBL). The UGT was fused to the

cDNA encoding TatC from *A. thaliana* and a 15-GS linker was added between TatC and the UGT to ensure some flexibility. The natural N-terminal P450s transmembrane domain was removed in the fusion proteins since the Tat proteins contain endogenous transmembrane domains. **c)** Schematic representation of the Tat-scaffolded dhurrin pathway in the thylakoid membrane in proximity of the highly abundant photosystem I complex. PSI, photosystem I; Fd, ferredoxin; FNR, ferredoxin-NAPH reductase.

Tat-fusion targets dhurrin pathway enzymes to thylakoid membranes

Western blot analysis using antibodies against CYP79A1, CYP71E1 and UGT85B1 were carried out on thylakoid membranes isolated from *N. benthamiana* leaves 5 days post *Agrobacterium*-mediated infiltration (Fig. 2.) to ensure correct localization of the Tat-fused enzymes.
The native *Sorghum* enzymes (U-79, U-71, U-UGT) fused to an N-terminal transit peptide from ferredoxin were used as controls [4]. In this experiment, constructs for each enzyme of the dhurrin pathway were infiltrated together in either UUU (previously described by Nielsen *et al* [4]) , SSC or LLC configurations, with letters denoting the N-terminal fusions of CYP79A1, CYP71E1 and UGT85B1, respectively (Table 1). Previously, U-UGT was shown to localize to stromal fractions and both U-79 and U-71 have been shown to insert into thylakoid membranes after translocation to the chloroplast via the fused transit peptide from ferredoxin [4]. As expected, both P450s were found in thylakoid membrane fractions, whether targeted via ferredoxin or TatB transit peptides (Fig. S1, see chloroplast fractionation method).

Construct combination	**CYP79 used**	**CYP71 used**	**UGT used**
UUU	U-79	U-71	U-UGT
SSC	BS-79	BS-71	C-UGT
LLC	BL-79	BL-71	C-UGT
LLU	BL-79	BL-71	U-UGT
UUC	U-79	U-71	C-UGT

Table 1 - Plasmid combinations infiltrated in leaves of *N. benthamiana*

The size differences of the P450 fusion enzymes (Fig. 2) arise due to the presence of either native transmembrane domain (U-79: 62 kDa), the presence of a short version of TatB (BS-79: 66 kDa) or a longer version of TatB (BL-79: 73 kDa). The same is valid for the CYP71E1 proteins, where U-71 is approximately 59 kDa, BS-71 is 62 kDa and BL-71 is 70 kDa. UGT85B1 fused to TatC (SSC and LLC) show thylakoid localization (C-UGT: 88 kDa) similar to the TatB-P450 fusions. Bands around 55 kDa (arrow) and 53 kDa (round arrow) can be seen on anti-

CYP71E1 and anti-UGT85B1 blots in the LLC and SSC construct combination (Fig. 2b and c). These sizes correspond approximately to those of enzymes without their respective N-terminal Tat fusions, which suggest that these fusion enzymes are proteolyzed to a limited extent.

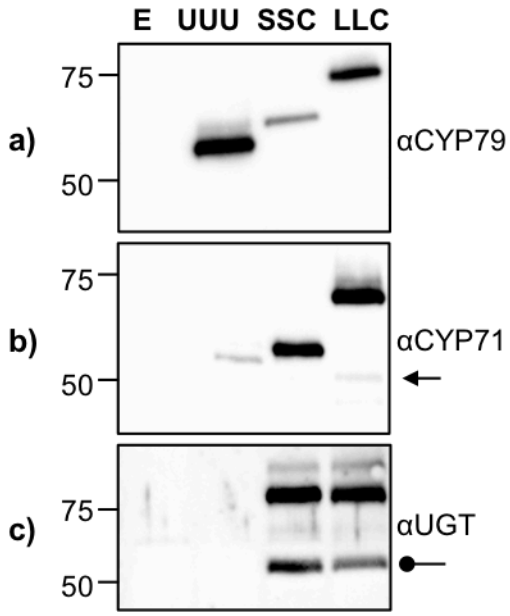

Fig. 2. Immunoblot analysis of thylakoids isolated from *N. benthamiana* leaves 5 days after *Agrobacterium* infiltration with fusion constructs. Membranes were probed with antibodies against (a) CYP79A1, (b) CYP71E1 or (c) UGT85B1. Mobility of protein standards of known mass (in kDa) are indicated on the left.

Tat-mediated scaffolding reduces pathway intermediates

We next wanted to investigate whether combinations of the Tat-fused enzymes showed improved channeling of tyrosine towards dhurrin *in vivo* compared to the native enzymes (Table1). To test this, we used LC-MS/MS on *N. benthamiana* leaves 5 days post *Agrobacterium*-mediated infiltration to analyze the production of dhurrin, its oxime and nitrile intermediates, as well as numerous glucosides resulting from improper channeling of intermediates through the pathway (Fig. 3). We could detect dhurrin, oxime and nitrile in all the experiments, showing that the P450s proteins are active when fused with both short and long TatB domains. We saw a clear reduction in the amount of both intermediates in both SSC and LLC

combinations, which led to almost complete disappearance of oxime peaks and 50% reduction in the amount of nitrile (Fig. 4) compared to the unmodified enzymes (UUU). Concurrently, dhurrin production increased from approximately 1300 mg/g FW to 4800 mg/g FW and 5300 mg/g FW for the SSC and LLC construct combinations, respectively. This could be due to the possible associations between the Tat proteins that in turn would bring the pathway enzymes into closer proximity and improve intermediate channeling to the next enzyme in the pathway. To clarify the relative importance of channeling of either oxime or nitrile through the pathway we performed control experiments using Tat-fused P450s with unfused UGT (LLU combination), or unfused P450s with Tat-fused UGT (UUC combination). The LLU combination serves to channel the oxime towards nitrile, and accordingly shows 84% reduction in the amount of oxime but no change of aldehyde or dhurrin levels. Conversely, in the UUC combination, wherein the UGT is anchored to the membrane should not have any channeling through the P450-catalyzed steps (tyrosine to nitrile), but improved channeling of nitrile to dhurrin. Consistent with our hypothesis, we found increased levels of oxime (63%) but a decrease in the level of nitrile (41%). Together with dhurrin production levels similar to the SSC and LLC combinations, this indicates that targeting of the UGT to the membrane is key to increase the channeling of the nitrile towards dhurrin.

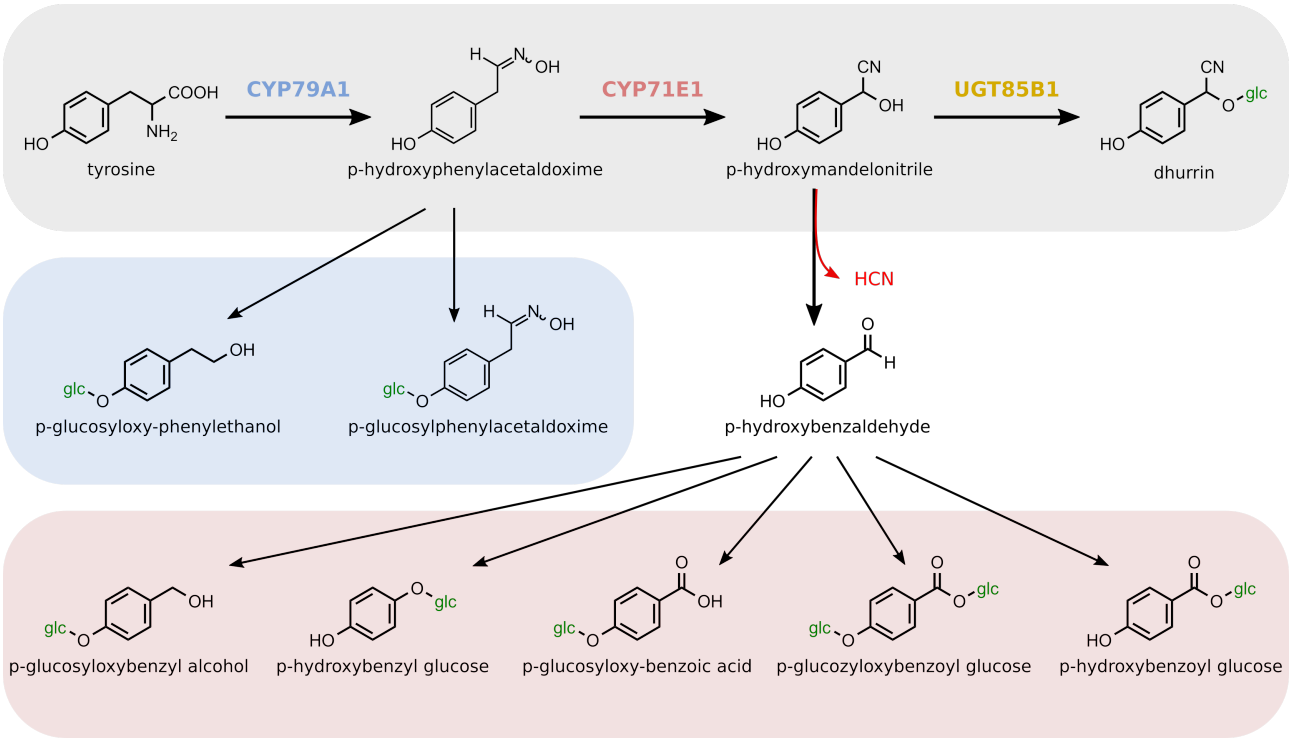

Fig. 3. Schematic representation of the dhurrin pathway and of the glycosylated products detected in *Nicotiana benthamiana*. The dhurrin pathway (grey) consists of two membrane-bound P450s (CYP79A1 and CYP71E1) and a soluble UDP-glucosyl transferase (UGT85B1). The intermediate *p*-hydroxymandelonitrile is labile and if not stabilized by the UGT dissociates into *p*-hydroxybenzaldehyde and hydrogen cyanide. Glycosylated products detected by LC-MS in transient expression of the pathway in *N. benthamiana* are derived from the intermediate *p*-hydroxyphenylacetaldoxime (oxime - in blue) or from *p*-hydroxybenzaldehyde (aldehyde - in red).

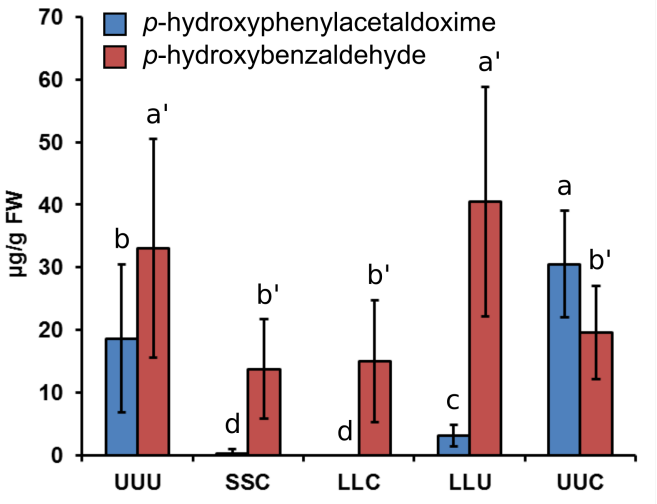

Construct combination	CYP79 used	CYP71 used	UGT used
UUU	U-79	U-71	U-UGT
SSC	BS-79	BS-71	C-UGT
LLC	BL-79	BL-71	C-UGT
LLU	BL-79	BL-79	U-UGT
UUC	U-79	U-71	C-UGT

Fig. 4. Quantification of dhurrin and intermediates: oxime and nitrile (detected as *p*-hydroxybenzaldehyde). The intermediate p-hydroxymandelonitrile is labile and it dissociates into hydrogen cyanide and the more stable and detectable aldehyde. See table for plasmids combination used for transient transformation of leaves. The amounts of intermediates are quantified relative to plant fresh weight (FW). Error bars ± SD. Different letters indicate a significant difference at $p < 0.05$ for each compound; asterisk, not-detected; N=14.

Tat-fusion reduces unwanted side products

Next we examined the production of glucosides derived from oxime and nitrile (Fig. 3) in plants infiltrated using the different plasmid combinations (Table1). Although these glucosides have been previously described [5,20,33] authentic standards were only available for some of them (Table S3), and we instead quantified the peak areas relative to that of an internal standard (amygdalin).

As shown in Fig. 5, we found a clear reduction in unwanted side products resulting from the Tat-enzyme fusions, with overall more dhurrin and fewer side products when both P450s and UGT carried N-terminal Tat-derived fusion domains. As reported above (Fig. 4), we saw 3.5 to 4-fold increase in dhurrin in SSC and LLC combinations, with overall levels of side-products reduced 5.5-fold and in some cases below the detection limit. The levels of oxime- but not nitrile-derived glucosides were reduced in the LLU combination, consistent with our hypothesis that fusion with the TatB-derived domains enables the CYP79A1 and CYP71E1 to channel the oxime towards nitrile more efficiently. Furthermore, UUC shows levels of dhurrin

formation comparable with those seen in the fully Tat-fused pathway (LLC), and increased the levels of glucosides derived from the oxime (Fig. 5, blue tones) but a clear reduction of the ones derived from nitrile (Fig. 5 red tones), which underscores the importance of close co-localization of UGT85B1 on the membrane for efficient channeling of nitrile towards dhurrin.

Fig. 5. Relative amounts of dhurrin and side products extracted from *N. benthamiana* leaves 5 days after infiltration (Next page). Plants were infiltrated with a combination of plasmids as indicated in the table. Quantification of peak areas is relative to the internal standard (amygdalin) and to plant fresh weight (FW). Further, metabolites in the plants infiltrated with the unmodified enzymes (UUU) were set to 100%. Error bars ± SD. Different letters indicate a significant difference at $p < 0.05$ for each compound; asterisk, not-detected; N=14.

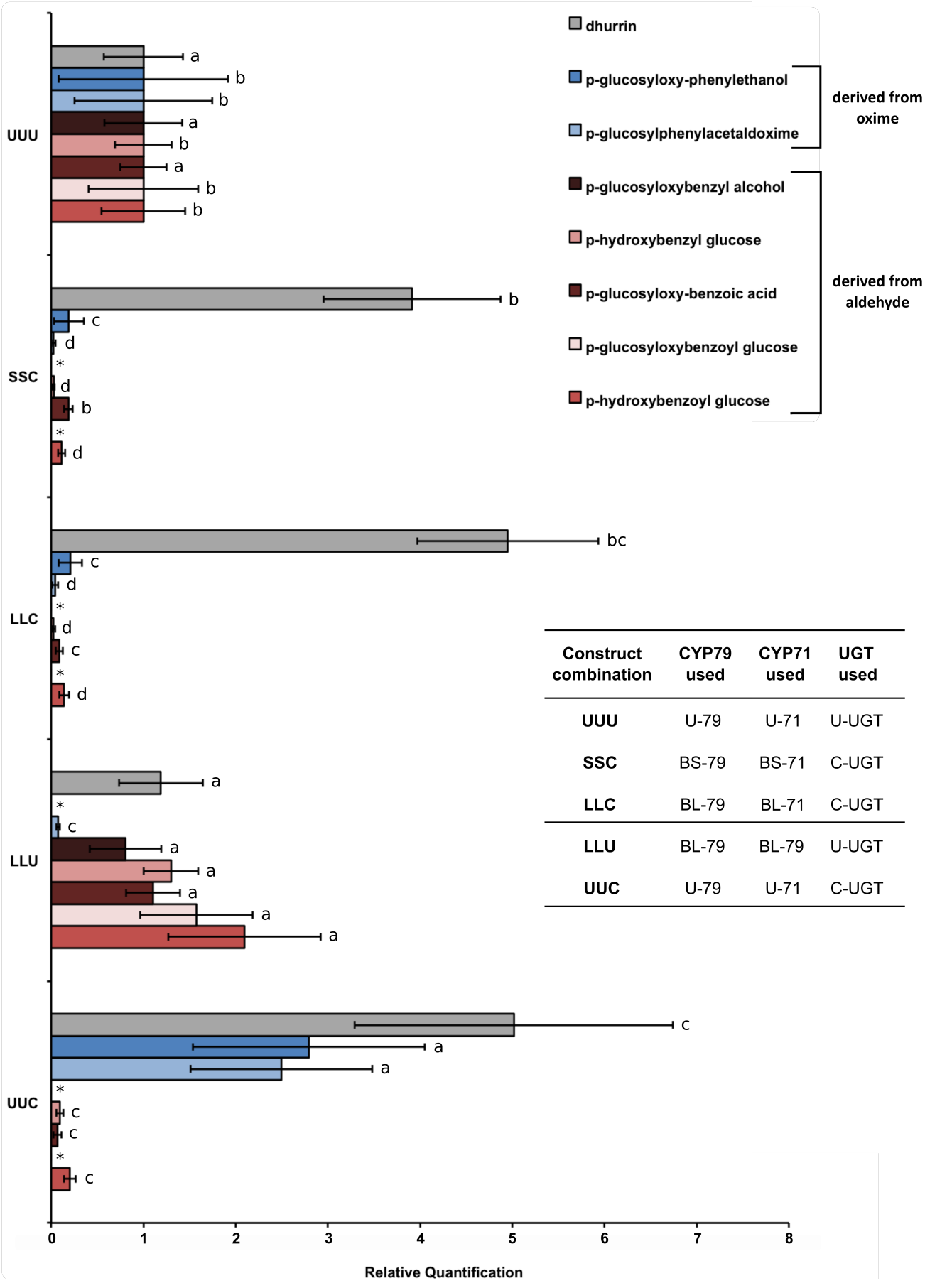

Construct combination	CYP79 used	CYP71 used	UGT used
UUU	U-79	U-71	U-UGT
SSC	BS-79	BS-71	C-UGT
LLC	BL-79	BL-71	C-UGT
LLU	BL-79	BL-79	U-UGT
UUC	U-79	U-71	C-UGT

1

Discussion and perspectives

This study shows a novel approach toward re-organizing a plant metabolic pathway in a non-native environment, in this case the chloroplast, by fusing the constituent enzymes with parts deriving from proteins of the Tat pathway, which are known to interact with each other [24,26–28]. Ensuring full orthogonality of the heterologous expressed proteins to avoid interaction with the endogenous ones is almost impossible to predict and only *in vivo* testing can show this. The rationale of choosing the Tat proteins from *Arabidopsis thaliana* was to ensure that the new "parts" would localize to the thylakoids of *N. benthamiana*.

All P450s fusions localize to the thylakoid fraction of the chloroplast (Fig. S1 and Fig. 2) as expected. Both TatB and TatC have their own transit peptide directing them to the chloroplast, and have been shown to localize to the thylakoid membranes [34,35]. The fusion of the P450s with the transit peptide from ferredoxin has previously been shown to localize them to the chloroplasts and the natural membrane domains of the P450s localize them to the thylakoid fraction [4].

Western blot analysis of proteins prepared from chloroplasts show that the fusion proteins have a higher susceptibility to proteolysis (see BL79, BL71 in Fig. S1) when compared to the same proteins in thylakoid membranes prepared directly without prior isolation of intact chloroplasts (Fig. 2). This could be due to the fact that the method to isolate thylakoids is much faster than the one to isolate chloroplasts thereby avoiding degradation by chloroplast proteases. Similar results have been described upon truncation of the transmembrane domain of CYP79A1 [33].

Triple infiltrations of leaves with UUU, SSC, and LLC led to expression differences in protein levels for the different pathway enzymes (Fig. 2). These might be due to internal protein regulation in the plants, possible related to the levels of side products formed. The unmodified enzymes (UUU), for example, have a high amount of glucosides derived from the aldehyde and a low expression of CYP71E1. This could be interpreted as a way to down regulate the amount of toxic side products formed. Similarly, SSC (where the P450s might not be interacting efficiently but where there is good channeling from the aldehyde to dhurrin) shows a low expression of CYP79A1 but not of CYP71E1.

The presence of all the enzymes of the pathway has been shown to be crucial for the reduction of side products and formation of a metabolon when expressed in the ER of Arabidopsis [21]. Translocation of the pathway from the ER to the chloroplast creates other obstacles, such as

the loss of a metabolon formation, which in turn leads to the loss of intermediates into competing pathways, with concomitant release of toxic hydrogen cyanide, and a loss of carbon that otherwise would be channeled into the final product (Fig. 3). This could be explained by the absence of the P450 oxido-reductase (POR), which has been shown to be important in the formation of the dhurrin metabolon in the ER of sorghum [36,37]. Alternatively it can be caused by the change of the lipid composition of the thylakoid membranes. Phospholipids such as phosphatidylcholine (PC) and phosphatidylinositol (PI) are the main components of the ER membrane while the thylakoid membranes are richer in galactolipids, such as monogalactosyldiacylglycerol (MGDG) and digalactosyldiacylglycerol (DGDG) [38]. The *in vitro* activity of CYP79A1 has been shown to be dependent on the type of phospholipid used for its reconstitution [9]. However, so far much less is known about the effect of the different thylakoid membrane composition on the P450s.

We found glucosides similar to the ones reported by both Bak *et al* and by Gnanasekaran *et al* [5,20] in tobacco, though we detected *p*-glucosyloxyphenylacetaldoxime but did not detect *p*-glucosyloxy-phenylacetonitrile and *p*-hydroxyphenyl-(acetaldoxime glucoside). These differences might arise because the studies used different LC- and GC-MS methods. Oxime has been shown to accumulate to levels 100–fold lower and be linearly correlated with its glucoside *p*-glucosylphenylacetaldoxime [33] upon expression of the first enzyme of the pathway, CYP79A1. We show only approximately (10-15)-fold lower levels, which could be explained by the fact that presence of all enzymes of the pathway efficiently consume the intermediates.

Likewise, observations made on *N. tabacum* stably expressing the dhurrin pathway[5], and the presence of numerous glucosides derived from nitrile in the leaf extracts of the unmodified pathway (the UUU combination) suggests inefficient coupling between the enzymes of the pathway. However, only glucosides derived from the oxime where detected when the pathway was expressed in the ER of *N. benthamina*[20]. This might suggest that stabilization of the nitrile by the UGT85B1 is the main step that is required for more efficient channeling when the pathway is transferred to the chloroplast. This could mean that CYP79A1 is more active in the ER or perhaps that the UGT is unstable in the chloroplast. Possibly its interaction with the P450s is hampered in some way by the new environment.

Both scaffolding strategies used, i.e. the SSC and LLC combinations, lead to an increase in dhurrin titers and a reduction in the accumulation of intermediates and unwanted side products, with LLC achieving the largest increase (Fig. 4 and 5).

The combinations LLU and UUC were performed to test if the previous results were an

outcome of channeling due to potential Tat-proteins interaction. The control used for the first step of the pathway, (LLU, where the P450s are fused to the long version of TatB but the UGT is soluble) shows a reduction in the amount of oxime and derived glucosides. It also displays a similar metabolic profile compared to the unmodified pathway (UUU) of dhurrin, nitrile and nitrile-derived glucosides. These results suggest that when the P450s are fused to the long versions of TatB, they come into close proximity, forming less oxime, but that its fusion has no influence on the final step of the pathway, once there is no TatC to promote interaction between the TatBs and subsequently between the P450s and the UGT.

Next, we wanted to see if the reduction in aldehyde, its glucosides and the increased production of dhurrin was simply due to the fact that we tethered the UGT to the membrane via TatC. By infiltrating the UUC combination, we targeted the UGT to the membrane, but no increased interaction should occur between the P450s and the UGT, besides their inherent ability to interact. This showed a similar increase in the levels of dhurrin compared to the LLC pathway and an equally steep reduction in nitrile and side products as also seen with the SSC and LLC combinations. However the levels of oxime and oxime-derived glucosides increased even in comparison with the unmodified pathway. We do not have a clear explanation of why this happens but studies with reconstituted liposomes have proposed that the UGT interacts specifically with both P450s, increasing the P450s catalytic properties and in the process increasing the flux and channeling from L-tyrosine to dhurrin [13]. It is probable that in the UUC combination a higher catalytic activity (probably caused by the proximity of the UGT on the membrane) would lead to more dhurrin and more oxime-derived products (since there is no proper channeling between the two P450s). In accordance with this, the results presented here seem to suggest that targeting the UGT to the membrane is one of the most important factors to achieve substrate channeling. Different permutations of the anchors/enzymes were not attempted but would be interesting to investigate in the future.

Previous work has shown that the dhurrin pathway can be relocated to the chloroplast of plants, cyanobacteria and algae [4–8,33], which allows the use of reducing power generated by photosynthesis. Likewise, the required precursors for dhurrin synthesis (tyrosine and UDP-glucose) are endogenously present in the chloroplast [39,40] and the reducing environment of the stroma may stabilize the P450s [4], making the chloroplast an attractive compartment for the production of bioactive natural products. Furthermore, chloroplasts appear to allow higher steady state accumulation of enzymes than heterologous expression and targeting to ER [20,21 5], which could further suggests that chloroplasts are well-suited compartments for high-level

expression of foreign enzymes.

In this project we used the tobacco transient expression system, which allows for fast heterologous protein expression and is widely used as a way to screen combinatorial testing [32,31]. Because of the fast experimental turnover of the method, no obvious interference with the endogenous Tat system was observed. These would be an important consideration to address in more prevalent production platform systems such as stable transformation of plants, since the new proteins could impair thylakoid functions. We did not attempt stable tobacco transformation since previous studies show that this is not a suitable system to express the dhurrin pathway [41]. Further, while not very prevalent yet, the transient expression system is becoming a common protein production platform system for commercial uses, especially for antibodies production and for vaccines such as ebola and influenza [31,42,43].

This study shows the first exchange of membrane anchors for an entire P450-dependent pathway used in plant chloroplasts. The dhurrin pathway was channeled by fusing its biosynthetic enzymes to components of the Twin-Arginine Translocation pathway, which have self-assembly properties that in turn allowed for co-localization of the pathway enzymes. Consequently, increased titers of dhurrin and a decrease of intermediates and side products were obtained. This strategy could *a priori* be transferred into other green hosts such as cyanobacteria and algae and allow future light-driven production of valuable compounds.

Materials and Methods

Vector Construction

Expression vectors containing the coding sequences for enzymes of the dhurrin pathway were constructed based on the high-expression pEAQ-HT vector [44].

Construction of the fusion of the ferredoxin transit peptide and the full-length enzymes (CYP79A1, CYP71E1 and UGT85B1) were carried out as previously described [4].

The full-length *Arabidopsis thaliana* TatB (HCF106 NCBI gene ID: 835320) and TatC (APG2 NCBI gene ID: 814640) genes were PCR-amplified form *A. thaliana* ecotype Columbia cDNA and cloned into *SalI-BamHI* linearized *E. coli* expression vector pUC19 for subsequent cloning steps. The Gibson assembly method [45] was used with the primers listed in Table S1.

The fusion constructs (TatBS-CYP79, TatBS-CYP71, TatBL-CYP79, TatBL-CYP71, TatC-UGT) were obtained from fragments amplified with Gibson-compatible overhangs from CYP79A1, CYP71E1, UGT85B1 [4],TatB and TatC with the primers listed in Table S2. Gene fragments were assembled into *AgeI-XhoI* linearized pEAQ vector using the Gibson assembly protocol (New England Biolabs). Correct assembly was confirmed by sequencing.

Agrobacterium infiltration of *N. benthamiana*

Wild type *N. benthamiana* plants were grown in a greenhouse under a 16/8 h light/dark cycle and day/night temperatures of 24/17ºC. Cells of *Agrobacterium tumefaciens* strain PGV3850 were transformed by electroporation in the presence of 2-10 ng vector in 2 mm cuvettes using a Gene Pulser (Bio-Rad) set to 400 Ω, 2.5 kV and 25 µF. Transformed cells were grown O/N at 28ºC, 220 rpm in YEP media containing 25 µg mL^{-1} rifampicin and 50 µg mL^{-1} kanamycin. Cells were concentrated by centrifugation at 4,000g for 15 min at RT and re-suspended in infiltration buffer (10mM MES, 10 mM $MgCl_2$, 200 µM acetosyringone) to a final OD_{600} of 0.4. Cells were shaken in infiltration buffer for 1-3h before infiltration of 4-6 week old plants with a syringe on the leaf underside. Post-infiltration plants were grown in the greenhouse for 5 days prior to isolation of chloroplasts or thylakoids, or extraction of metabolites.

Thylakoid isolation

Thylakoid membranes were isolated from *N. benthamiana* leaves 5 days after *Agrobacterium* infiltration. All steps were carried out on ice and under green light. Leaves were homogenized in homogenization buffer (400 mM sucrose, 5 mM $MgCl_2$, 10 mM NaCl, 20 mM tricine (pH 7.5),

100mM sodium ascorbate, 5 mg mL-1 BSA) and filtered through 2 layers of nylon mesh (5 µm). Chloroplasts were sedimented at 5,000*g* for 10 min and lysed by resuspension in 5mM tricine (pH 7.9) for 15 min. Subsequently, thylakoids were sedimented at 11,200*g* for 10 min and resuspended in homogenizing buffer without sodium ascorbate and BSA but supplemented with 20% (v/v) glycerol. Chlorophyll content was determined in 80% acetone according to Lichtenthaler [46]. Thylakoid membranes were snap frozen in liquid N2 and stored (-80%) until further use.

Chloroplast isolation and fractionation

Intact chloroplasts were isolated from *N. benthamiana* leaves 5 days after *Agrobacterium* infiltration. All steps were carried out on ice and under green light. Leaves were homogenized in HS buffer (50 mM Hepes – KOH pH 8, 0.33 M sorbitol) and filtrated through 2 layers of nylon mesh (5 µm). Homogenate was sedimented at 3,300*g* for 2 min. The chloroplast pellet was gently resuspended in HS buffer and layered onto Percoll pads (40% Percoll in 50 mM Hepes – KOH pH 8, 0.33 M sorbitol) and centrifuged at 1,400*g* for 8 min to fractionate intact and broken chloroplasts. Sedimented intact chloroplasts were washed in HS buffer and re-sedimented at 3000*g* for 2 min and resuspended in HS buffer. For fractionation of chloroplasts into stroma and thylakoid fractions, aliquots of purified intact chloroplasts were diluted fourfold with 5 mM tricine (pH 7.9) and allowed to lyse for 15 min on ice. Thylakoid membranes were then pelleted by centrifugation (11,200*g*, 10 min), and the stromal fraction recovered as the supernatant. The pellet was washed three times by resuspending in excess HS buffer and sedimenting by centrifugation (11,200*g*, 10 min) and finally resuspended in 5 mM tricine (pH 7.9).

Immunoblotting

Thylakoid proteins were separated by SDS-Page on 12% TGX stain-free gels (Bio-Rad) at 250 V for 25-30 min in TRIS-glycine-SDS running buffer (Bio-Rad). Proteins were then transferred onto PVDF membranes (Bio-Rad) at 2.5 A for 7 min using a Trans-Blot Turbo blotting system (Bio-Rad). Membranes were blocked for 1 h at room temperature in 5% skimmed milk in PBS + 0.005% Tween-20 (PBS-T), washed and incubated O/N with primary antibodies against either CYP79A1 (1:3000), CYP71E1 (1:3000) or UGT85B1 (1:3000) in PBS-T with 2% skimmed milk. Blots were then washed in PBS-T and subsequently incubated for 1 h at RT with polyclonal swine anti-rabbit immunoglobulins conjugated to HRP (DAKO) (1:5000) in PBS-T with 2%

skimmed milk. Secondary antibody was detected with Super Signal West Dura substrate (Thermo Scientific) using a ChemiDoc MP imaging system using a cooled CCD camera (Bio-Rad) set to automatic exposure setting. Total Protein was visualized on the membranes using the stain-free blot setting.

Extraction of metabolites for LC-MS analysis

Four leaf discs were made from infiltrated *N. benthamiana* leaves with a 1cm cork borer. Leaf discs were weighed, placed in a 1.5 mL tube together with 2 chrome ball-bearings and frozen in liquid N2. Samples were homogenized in a mixer mill (Retsch) for 1 min 30 sec. Samples were centrifuged (4,300*g*, 3 min), 0.5 mL 80% methanol was added and the material was re-suspended and extracted by vortexing (5 min, RT). Samples were centrifuged (5 min, 10,000*g*) and the supernatant was filtered through centrifugal filters (0.2 µm PTFE membrane, Advantec) and stored at -20ºC. Samples were further diluted to 20% methanol and filtered through centrifugal filters again (0.2 µm PTFE membrane, Advantec) and further diluted according to the LC-MS method.

LC-MS/MS analysis of *p*-hydroxyphenylacetaldoxime, *p*-glucosyloxyphenylacetaldoxime and *p*-hydroxybenzaldehyde

Quantification of *p*-hydroxyphenylacetaldoxime, *p*-glucosyloxyphenylacetaldoxime and *p*-hydroxybenzaldehyde was carried out on a Bruker EVOQ Elite UPLC-coupled triple quadrupole MS/MS system. Chromatography was performed on a Kinetex Biphenyl column (Phenomenex, 1.7 µm, 100 Å, 2.1x100 mm) at a flow rate of 400 µl min^{-1} with an oven temperature of 40 °C. A gradient between A: 2 mM ammonium acetate (pH 6.6) and B: 100% methanol was developed as follows: 0-0.3 min isocratic 10% B; 0.3-5 min 10-25% B; 5-5.1 min 25-98% B, 6.1-6.2 min 98-10% B; 6.2-8.5 min isocratic 10% B. Ionization was carried out in negative ESI mode for *p*-hydroxyphenylacetaldoxime and *p*-hydroxybenzaldehyde or in positive ESI mode for *p*-glucosyloxyphenylacetaldoxime, with a probe temperature of 300 °C and a spray voltage of -4500 V or +3000 V. *p*-Hydroxyphenylacetaldoxime was detected using selected ion monitoring at an *m/z* of (-)150, with *E* and *Z* isomers eluting at t_R of 4.2 and 4.6 min respectively, while *p*-glucosyloxyphenylacetaldoxime and *p*-hydroxybenzaldehyde were detected by multiple reaction monitoring of m/z (+)314>152 transitions (10 eV collision energy) for the glucoside, with *E* and *Z* isomers eluting at 2.8 and 3.0 min, and m/z (-)121>92 transitions (16 eV collision energy) for the aldehyde, eluting at t_R of 4.5 min. Standard curves of *p*-

hydroxyphenylacetaldoxime, *p*-glucosyloxyphenylacetaldoxime and *p*-hydroxybenzaldehyde ranging from 50 to 2000, 50 to 10000 and 5-2000 µg L^{-1} were made using authentic standards diluted into 10% methanolic extracts from non-infiltrated tobacco leaf discs.

LC-MS/MS analysis of Dhurrin and glucosides

For the LC-MS analysis a 1200 Series HPLC (Agilent) was coupled by the ESI-Source to a HCT plus ion trap instrument (Bruker). The metabolites were separated on a Zorbax 300 SB-C18 column (Agilent) at a flow rate of 200 µl min^{-1} using a gradient between A: H2O, 0.05% formic acid, 10 µM NaCl and B: 99.95% Acetonitrile, 0.05% formic acid as follows: 0-8 min 2-40% B, 8-9 min 40-90% B, 9-14 min isocratic 90%, 14-18 min 2% B. The mass spectrometer was set to Ultrascan positive ion mode with a mass range of 100-8.00 m/z. MS/MS was carried out on the most abundant peaks in the full scan, with a dynamic exclusion activated after 2 spectra and released again after 0.5 min. Standard curves of dhurrin, *p*-glucosylphenylacetaldoxime, *p*-glucosyloxy-phenylethanol and *p*-glucosyloxy-benzoic acid ranging from 100 to 20000 µg L^{-1} were made using authentic standards diluted into 20% methanolic extracts from non-infiltrated tobacco leaf discs.

Statistics

Normal distribution of data for each condition was evaluated with the Shapiro-Wilk Normality Test. When normality was validated with $P<0.05$, t-test pairwise comparisons were calculated to determine statistical significance. When data did not satisfy the normality law, Mann-whitney Rank Sum t-test comparisons were calculated. Pairwise comparisons with $P<0.05$ were considered as significant. All statistical analysis were performed using Sigmaplot.

Acknowledgements

The authors acknowledge financial support from 1) Copenhagen Plant Science Centre, 2) the Center for Synthetic Biology "bioSYNergy" funded by the UCPH Excellence Programme for Interdisciplinary Research, 3) from "Plant Power: Light-Driven Synthesis of Complex Terpenoids Using Cytochromes P450" (12-131834) funded by Innovation Fund Denmark (previously the Danish Council for Strategic Research), 4) from the Novo Nordisk Foundation (Sustainable production of forskolin, a high-value diterpenoid, NNF13OC0005685) and 5) the VILLUM Foundation (Light-driven biosynthesis: Improving photosynthesis by designing and exploring novel electron transfer pathways, Project no. 13363).

We would also like to thank Professor Mohammed Saddik Motawia for providing all the chemical standards for LC-MS.

References

1. Lindberg Møller, B. Disruptive innovation: channeling photosynthetic electron flow into light- driven synthesis of high-value products. / *Synth. Biol.* **1,** 330–359 (2014).
2. Nielsen, A. Z. *et al.* Extending the biosynthetic repertoires of cyanobacteria and chloroplasts. *Plant J.* (2016). doi:10.1111/tpj.13173
3. Lassen, L. M. *et al.* Redirecting photosynthetic electron flow into light-driven synthesis of alternative products including high-value bioactive natural compounds. *ACS Synth. Biol.* **3,** 1–12 (2014).
4. Nielsen, A. Z. *et al.* Redirecting Photosynthetic Reducing Power toward Bioactive Natural Product Synthesis. *ACS Synth. Biol.* **2,** 308–315 (2013).
5. Gnanasekaran, T. *et al.* Transfer of the cytochrome P450-dependent dhurrin pathway from Sorghum bicolor into Nicotiana tabacum chloroplasts for light-driven synthesis. *J. Exp. Bot.* **67,** 2495–506 (2016).
6. Wlodarczyk, A. *et al.* Metabolic engineering of light-driven cytochrome P450 dependent pathways into Synechocystis sp. PCC 6803. *Metab. Eng.* **33,** 1–11 (2016).
7. Lassen, L. M. *et al.* Anchoring a plant cytochrome P450 via PsaM to the thylakoids in Synechococcus sp. PCC 7002: evidence for light-driven biosynthesis. *PLoS One* **9,** e102184 (2014).
8. Gangl, D. *et al.* Expression and membrane-targeting of an active plant cytochrome P450 in the chloroplast of the green alga Chlamydomonas reinhardtii. *Phytochemistry* **110,** 22–8 (2015).
9. Sibbesen, O., Koch, B., Halkier, B. A. & Møller, B. L. Cytochrome P-450TYR is a multifunctional heme-thiolate enzyme catalyzing the conversion of L-tyrosine to p-hydroxyphenylacetaldehyde oxime in the biosynthesis of the cyanogenic glucoside dhurrin in Sorghum bicolor (L.) Moench. *J. Biol. Chem.* **270,** 3506–11 (1995).
10. Kahn, R. A., Bak, S., Svendsen, I., Halkier, B. A. & Møller, B. L. Isolation and reconstitution of cytochrome P450ox and in vitro reconstitution of the entire biosynthetic pathway of the cyanogenic glucoside dhurrin from sorghum. *Plant Physiol.* **115,** 1661–70 (1997).
11. Jones, P. R., Moller, B. L. & Hoj, P. B. The UDP-glucose:p-hydroxymandelonitrile-O-glucosyltransferase that catalyzes the last step in synthesis of the cyanogenic glucoside dhurrin in Sorghum bicolor. Isolation, cloning, heterologous expression, and substrate specificity. *J. Biol. Chem.* **274,** 35483–91 (1999).

12. Gleadow, R. M. & Møller, B. L. Cyanogenic glycosides: synthesis, physiology, and phenotypic plasticity. *Annu. Rev. Plant Biol.* **65,** 155–85 (2014).
13. Laursen, T. *et al.* Characterization of a dynamic metabolon producing the defense compound dhurrin in sorghum. *Science (80-.).* **354,** (2016).
14. Jensen, K. & Møller, B. L. Plant NADPH-cytochrome P450 oxidoreductases. *Phytochemistry* **71,** 132–141 (2010).
15. Jensen, K., Jensen, P. E. & Møller, B. L. Light-driven chemical synthesis. *Trends Plant Sci.* **17,** 60–3 (2012).
16. Dueber, J. E. *et al.* Synthetic protein scaffolds provide modular control over metabolic flux. *Nat. Biotechnol.* **27,** 753–759 (2009).
17. Conrado, R. J., Varner, J. D. & DeLisa, M. P. Engineering the spatial organization of metabolic enzymes: mimicking nature's synergy. *Curr. Opin. Biotechnol.* **19,** 492–9 (2008).
18. Laursen, T., Lindberg Møller, B. & Bassard, J.-E. Plasticity of specialized metabolism as mediated by dynamic metabolons. *Trends Plant Sci.* **20,** 20–32 (2015).
19. Pröschel, M., Detsch, R., Boccaccini, A. R. & Sonnewald, U. Engineering of Metabolic Pathways by Artificial Enzyme Channels. *Front. Bioeng. Biotechnol.* **3,** 168 (2015).
20. Bak, S., Olsen, C. E., Halkier, B. A. & Møller, B. L. Transgenic tobacco and Arabidopsis plants expressing the two multifunctional sorghum cytochrome P450 enzymes, CYP79A1 and CYP71E1, are cyanogenic and accumulate metabolites derived from intermediates in Dhurrin biosynthesis. *Plant Physiol.* **123,** 1437–48 (2000).
21. Kristensen, C. *et al.* Metabolic engineering of dhurrin in transgenic Arabidopsis plants with marginal inadvertent effects on the metabolome and transcriptome. *Proc. Natl. Acad. Sci. U. S. A.* **102,** 1779–84 (2005).
22. Patel, R., Smith, S. M. & Robinson, C. Protein transport by the bacterial Tat pathway. *Biochim. Biophys. Acta* **1843,** 1620–8 (2014).
23. Palmer, T. & Berks, B. C. The twin-arginine translocation (Tat) protein export pathway. *Nat. Rev. Microbiol.* **10,** 483–96 (2012).
24. Maldonado, B. *et al.* Characterisation of the membrane-extrinsic domain of the TatB component of the twin arginine protein translocase. *FEBS Lett.* **585,** 478–484 (2011).
25. Zhang, Y., Wang, L., Hu, Y. & Jin, C. Solution structure of the TatB component of the twin-arginine translocation system. *Biochim. Biophys. Acta* **1838,** 1881–8 (2014).
26. Kneuper, H. *et al.* Molecular dissection of TatC defines critical regions essential for

protein transport and a TatB-TatC contact site. *Mol. Microbiol.* **85,** 945–61 (2012).
27. Rollauer, S. E. *et al.* Structure of the TatC core of the twin-arginine protein transport system. *Nature* **492,** 210–4 (2012).
28. Bolhuis, A., Mathers, J. E., Thomas, J. D., Barrett, C. M. & Robinson, C. TatB and TatC form a functional and structural unit of the twin-arginine translocase from Escherichia coli. *J. Biol. Chem.* **276,** 20213–9 (2001).
29. Lee, P. A. *et al.* Cysteine-scanning mutagenesis and disulfide mapping studies of the conserved domain of the twin-arginine translocase TatB component. *J. Biol. Chem.* **281,** 34072–85 (2006).
30. Priyanka, V., Chichili, R., Kumar, V. & Sivaraman, J. REVIEWS Linkers in the structural biology of protein–protein interactions. (2012). doi:10.1002/pro.2206
31. Powell, J. & D., J. From Pandemic Preparedness to Biofuel Production: Tobacco Finds Its Biotechnology Niche in North America. *Agriculture* **5,** 901–917 (2015).
32. Sparkes, I. A., Runions, J., Kearns, A. & Hawes, C. Rapid, transient expression of fluorescent fusion proteins in tobacco plants and generation of stably transformed plants. *Nat. Protoc.* **1,** 2019–2025 (2006).
33. Mellor, S. B. *et al.* Fusion of Ferredoxin and Cytochrome P450 Enables Direct Light-Driven Biosynthesis. *ACS Chem. Biol.* (2016). doi:10.1021/acschembio.6b00190
34. Cline, K. & Mori, H. Thylakoid Δ pH-dependent precursor proteins bind to a cpTatC–Hcf106 complex before Tha4-dependent transport. *J. Cell Biol.* **0871911,** 21–9525 (2001).
35. Martin, J. R., Harwood, J. H., Mccaffery, M. W., Fernandez, D. E. & Cline, K. C. Localization and integration of thylakoid protein translocase subunit cpTatC. *Plant J* **58,** 831–842 (2009).
36. Nielsen, K. A., Tattersall, D. B., Jones, P. R. & M??ller, B. L. Metabolon formation in dhurrin biosynthesis. *Phytochemistry* **69,** 88–98 (2008).
37. Laursen, T., Jensen, K. & Møller, B. L. Conformational changes of the NADPH-dependent cytochrome P450 reductase in the course of electron transfer to cytochromes P450. *Biochim. Biophys. Acta - Proteins Proteomics* **1814,** 132–138 (2011).
38. Dörmann, P. & Benning, C. Galactolipids rule in seed plants. *Trends Plant Sci.* **7,** 112–118 (2002).
39. Rippert, P., Puyaubert, J., Grisollet, D., Derrier, L. & Matringe, M. Tyrosine and phenylalanine are synthesized within the plastids in Arabidopsis. *Plant Physiol.* **149,**

1251–60 (2009).
40. Okazaki, Y. *et al.* A chloroplastic UDP-glucose pyrophosphorylase from Arabidopsis is the committed enzyme for the first step of sulfolipid biosynthesis. *Plant Cell* **21,** 892–909 (2009).
41. Gnanasekaran, T. *et al.* Transfer of the cytochrome P450-dependent dhurrin pathway from Sorghum bicolor into Nicotiana tabacum chloroplasts for light-driven synthesis. *J. Exp. Bot.* **67,** 2495–506 (2016).
42. Tusé, D., Tu, T. & McDonald, K. A. Manufacturing economics of plant-made biologics: case studies in therapeutic and industrial enzymes. *Biomed Res. Int.* **2014,** 256135 (2014).
43. Marsian, J. *et al.* Plant-made polio type 3 stabilized VLPs—a candidate synthetic polio vaccine. *Nat. Commun.* **8,** 245 (2017).
44. Sainsbury, F., Thuenemann, E. C. & Lomonossoff, G. P. pEAQ: versatile expression vectors for easy and quick transient expression of heterologous proteins in plants. *Plant Biotechnol. J.* **7,** 682–693 (2009).
45. Gibson, D. G. *et al.* Enzymatic assembly of DNA molecules up to several hundred kilobases. *Nat. Methods* **6,** 343–345 (2009).
46. Lichtenthaler, H. K. [34] Chlorophylls and carotenoids: Pigments of photosynthetic biomembranes. *Methods Enzymol.* **148,** 350–382 (1987).

Supplementary Information

Construct	F/R	Sequence
TatB	F	AGTGGATCCTCAATCTTGCCTTGGAGGAGAT
	R	ACTGTCGACATGGCCATGGCGTTACAGATTA
TatC	F	AGTGGATCCTCACCGACCTGTGAGCTTGAC
	R	ACTGTCGACATGAGCAGCACAAGCACTAGTT

Table S1. Primers used for Isolation from cDNA from A. thaliana into pUC19

Construct	Fragment	F/R	Sequence
TatBs-CYP79	TatBs	F	TATTCTGCCCAAATTCGCGACCGGTATGGCCATGGCGTTACAGATTA
		R	GGCTCGGGCCAGGTAGATATCATCAAGGCCAATTTCAC
	CYP79	F	AAATTGGCCTTGATGATATCTACCTGGCCCGAGCCCTGA
		R	GAAACCAGAGTTAAAGGCCTCGAGTCAGATGGAGATGGACGGGTA
TatBs-CYP71	TatBs	F	TATTCTGCCCAAATTCGCGACCGGTATGGCCATGGCGTTACAGATTA
		R	CTGTTCCTGCTCCTGCTGATATCATCAAGGCCAATTTCAC
	CYP71	F	AAATTGGCCTTGATGATATCAGCAGGAGCAGGAACAGGAG
		R	GAAACCAGAGTTAAAGGCCTCGAGCTAGGCGGCGCGGCGGTT
TatBL-CYP79	TatBL	F	TATTCTGCCCAAATTCGCGACCGGTATGGCCATGGCGTTACAGATTA
		R	GGGCTCGGGCCAGGTATGTTTGGCTTTCAGCGGGAGA
	CYP79	F	CCCGCTGAAAGCCAAACATACCTGGCCCGAGCCCTGA
		R	GAAACCAGAGTTAAAGGCCTCGAGTCAGATGGAGATGGACGGGTA
TatBL-CYP71	TatBL	F	TATTCTGCCCAAATTCGCGACCGGTATGGCCATGGCGTTACAGATTA
		R	CTGTTCCTGCTCCTGCTTGTTTGGCTTTCAGCGGGAGA
	CYP71	F	CCCGCTGAAAGCCAAACAAGCAGGAGCAGGAACAGGAG
		R	GAAACCAGAGTTAAAGGCCTCGAGCTAGGCGGCGCGGCGGTT

TatC-UGT	**TatC**	**F**	TATTCTGCCCAAATTCGCGACCGGTATGAGCAGCACAAGCACTCGT
		R	AGATGCACCTCCACCTGATCCACCTCCACCAGAACCACCTCCAGTCCGACCTGTGAGCTTGAC
	UGT	**F**	ACTGGAGGTGGTTCTGGTGGAGGTGGATCAGGTGGAGGTGCATCTATGGGCAGCAACGCGCCGC
		R	GAAACCAGAGTTAAAGGCCTCGAGTCACTGCTTGCCCCCGACC

Table S2. Primers used for PCR amplification of fragments for Gibson Assembly

Constructs	Amount of compound in ug/g FW (+/- SD)		
	***p*-glucosylphenyl--acetaldoxime**	***p*-glucosyloxy-phenylethanol**	***p*-glucosyloxy-benzoic acid**
UUU	20.2 (156.7)	148.7 (141.5)	1152.9 (282.3)
SSC	6.1 (4.2)	25.8 (24.9)	160.5 (60.5)
LLC	9.5 (6.5)	23.6 (14.5)	35.7 (31.5)
LLU	15.7 (4.5)	*	952.5 (237.7)
UUC	503.9 (206.4)	281.3 (120.9)	26.7 (15.3)

Table S3. Absolute quantification of *p*-glucosylphenylacetaldoxime; *p*-glucosyloxy-phenylethanol and *p*-glucosyloxy-benzoic acid from triple infiltrated plants. Asterisk, not-detected; N=14.

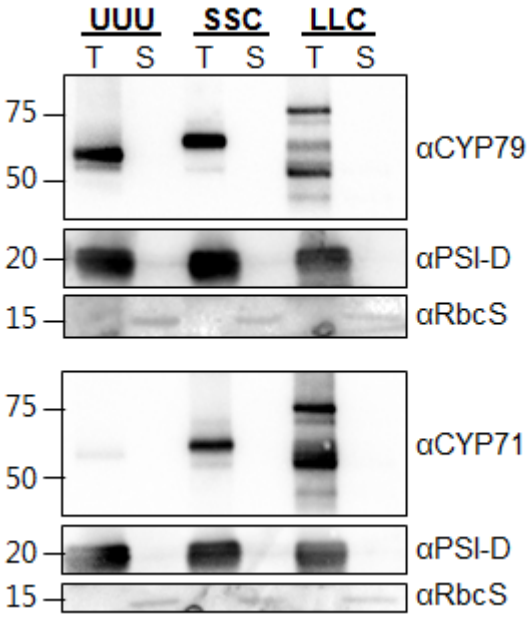

Fig. S1. – Immunoblot analysis of chloroplasts isolated from tobacco leaves 5 days after agroinfiltration and fractionated into thylakoid (T) and stroma (S) fractions. Membranes were probed with antibodies against either CYP79A1, CYP71E1, PSI-D (PsaD, a thylakoid marker), or a RuBisCo small subunit (RbcS, a stroma marker). Mobilities of protein standards of known mass (in kDa) are indicated on the left.